

Robust Optimization for A 6.78-MHz Wireless Power Transfer System with Class E Rectifier

Ming Liu¹, *Student Member, IEEE*, Yue Qiao², Chengbin Ma¹, *Member, IEEE*

1. Univ. of Michigan-Shanghai Jiao Tong Univ. Joint Institute,

Shanghai Jiao Tong University, Shanghai, P. R. China

2. GE AVIC Civil Avionics Systems Company Limited, Shanghai, P. R. China

Email: mikeliu@sjtu.edu.cn, chimmy.qiao@aviagesystems.com, chbma@sjtu.edu.cn

Abstract—Class E rectifier is suitable for high-frequency rectification due to its soft-switching operation, which potentially improves the efficiency of wireless power transfer (WPT) systems working at MHz. In this paper, a robust optimization design is discussed for a 6.78-MHz WPT system using the Class E rectifier. In real WPT applications, the parameter variations are possible to be originated from the misalignment of coils, the change of load, and the varying equivalent resistance of rectifying diode under different power level. In this case, a robust optimization problem is formulated to find a solution of system design variables that is both optimal and insensitive to uncertainty of parameters. A genetic-based inner-outer algorithm is applied to solve this problem, where an explicit trade-off among efficiency and robustness is demonstrated in the optimization results. In the final experiments, the analytical results are proved to well match the experimental results. Compared with the WPT system using the conventional design, the proposed robust optimization can achieve an improved design with high efficiency, which is also robust against the variations of working conditions.

I. INTRODUCTION

Wireless power transfer (WPT) at megahertz (MHz) is now being considered a promising candidate for the mid-range transfer of a medium amount of power [1], [2]. It is because generally a higher operating frequency (such as 6.78 and 13.56 MHz) is desirable for a more compact and lighter WPT system with a longer transfer distance. Lots of researches have been done on the design and optimization of WPT systems both at component and system levels, including the improvements on coupling coils [3]–[6], power amplifier (PA) [7], [8], and load control [9], [10].

Due to soft-switching operation, the Class E rectifier is a promising candidate for high frequency rectifications. The application of the Class E rectifier in WPT system was first investigated at an operating frequency of 800 KHz and an efficiency of 94.43% was reported in [11]. A state-space-based analysis of the class E^2 converter for WPT is presented in [12]. In the aforementioned applications of Class E rectifier in WPT systems, the resonant coils and rectifier are discussed separately, where the resonance between coils is empirically designed without consideration of the rectifier impedance. However, the appearance of the input reactance of rectifier cannot be neglected because it would detune the coupling coils from the resonance especially when the working frequency is as high as MHz. Meanwhile, in real WPT applications, the variations of working conditions are commonly existed,

including the misalignment of coupling coils, the change of DC load, and the varying equivalent resistance of diode under different power level. Instead of addressing the peak efficiency for power transmission, a compromised design with relatively stable performance may be more desirable in consideration of all the unpredictable variations of working conditions, namely the robust optimization design.

Therefore, this paper devotes to the analysis and robust optimization of a 6.78-MHz WPT system with a Class E current-driven rectifier against the varying working condition. Firstly, the input impedance of the Class E rectifier is analytically derived considering the on-resistance of the rectifying diode, its forward voltage drop, and the equivalent series resistance (ESR) of the filter inductor. Then the efficiency of the overall WPT system including coupling coils and rectifier is further formulated based on the input impedance of the Class E rectifier. Using the analytical formulation of system efficiency, the robust optimization design for the MHz WPT is provided considering the variations of mutual inductance coefficient, load resistance, and the equivalent parasitic resistance of the diode. The theoretical design is finally validated in experiment by using a 6.78-MHz wireless power transfer system. The experimental results shows that the WPT system using the proposed robust optimization can achieve the higher robustness than that of the conventional design under the varying work conditions.

II. MODELING AND ANALYSIS

The entire configuration of a 6.78-MHz WPT system is demonstrated in Fig. 1, including a power amplifier, coupling coil, and Class E rectifier. In this circuit, the power amplifier are regarded as a 6.78 MHz power source. The efficiency of the overall system is formulated analytically through circuit analysis of coupling coils and rectifier, considering the power loss in the self-resistances of coupling coils, on-resistance of the rectifying diode, and equivalent series resistance (ESR) of the filter inductor. The variations of system model are further defined as interval-based uncertainties for robustness analysis, in corresponds to the misalignment of coupling coils, the changing of load together with the varying equivalent resistance of rectifying diode.

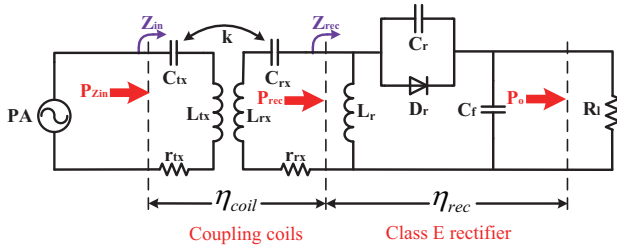


Fig. 1. Circuit topology of the overall WPT system.

A. Current-driven Class E rectifier

The circuit of the current-driven Class E rectifier in Fig. 1 consists of a DC filter inductor L_r , rectifying diode D_r , a parallel capacitor C_r , and a filter capacitor C_f . The rectifier is driven by a sinusoidal current source i_{rec} and the output current to the DC load R_l is I_0 . The equivalent circuit of the rectifier is demonstrated in Fig. 2, where r_{L_r} is used to denote the equivalent series resistance (ESR) of the inductor L_r . The rectifying diode D_r can be modeled as combination of forward voltage drop and on-resistance in the on-state. The equivalent resistance of the diode is defined as r_{D_r} in consideration of both the forward voltage drop and on-resistance. Note the input impedance of the Class E rectifier can be derived by modeling the diode as a equivalent resistance but out the combination of forward voltage drop and on-resistance.

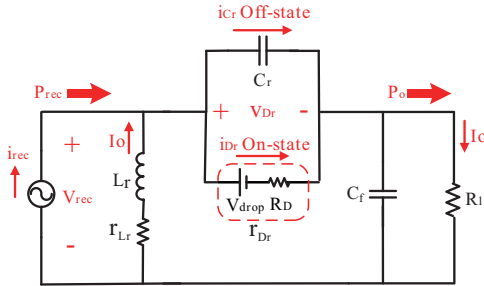


Fig. 2. Circuit model of the Class E rectifier.

Typically, the filter inductor L_r and filter capacitor C_f in Class E rectifier are regarded as infinite large. The output current I_0 is then assumed to have a constant value, i.e. DC current. Suppose the input current i_{rec} is pure sinusoidal with operating frequency ω and initial phase ϕ_{rec} ,

$$i_{rec} = I_m \sin(\omega t + \phi_{rec}). \quad (1)$$

As shown in Fig. 3, the diode is on the off-state when $0 < \omega t \leq 2\pi(1-D)$, where D is defined as the duty cycle of the diode. The current across the diode i_{D_r} can be represented as

$$i_{D_r} = \begin{cases} 0 & \omega t \in (0, 2\pi(1-D)] \\ I_m \sin(\omega t + \phi_{rec}) + I_0 & \omega t \in (2\pi(1-D), 2\pi]. \end{cases} \quad (2)$$

Similarly, the current across the parallel capacitor C_r can also be represented as a similar form.

$$i_{C_r} = \begin{cases} I_m \sin(\omega t + \phi_{rec}) + I_0 & \omega t \in (0, 2\pi(1-D)] \\ 0 & \omega t \in (2\pi(1-D), 2\pi]. \end{cases} \quad (3)$$

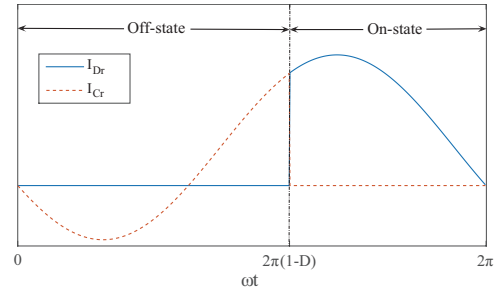


Fig. 3. The ideal current waveforms across the diode and capacitor in one cycle.

Since i_{D_r} is zero during the switching condition of diode, i.e., $\omega t = 2n\pi$ in (2), I_0 can be solved as

$$I_0 = -I_m \sin \phi_{rec}. \quad (4)$$

Hence, the on-state current of the diode is

$$i_{D_r} = I_m [\sin(\omega t + \phi_{rec}) - \sin \phi_{rec}], \quad \omega t \in (2\pi(1-D), 2\pi]. \quad (5)$$

The voltage across the diode (v_{D_r}) can be defined as a piecewise continuous function

$$v_{D_r} = \begin{cases} v_{D_r,off} & \text{when } 0 < \omega t \leq 2\pi(1-D) \\ v_{D_r,on} & \text{when } 2\pi(1-D) < \omega t \leq 2\pi. \end{cases} \quad (6)$$

Then, the off-state voltage $v_{D_r,off}$ and on-state voltage $v_{D_r,on}$ can be derived according to (3) and (5).

$$v_{D_r,off} = \frac{1}{C_r} \int_0^t i_{C_r} dt, \\ v_{D_r,on} = i_{D_r} \cdot r_{D_r},$$

$$v_{D_r,off} = \frac{I_m}{\omega C_r} [\cos \phi_{rec} - \cos(\omega t + \phi_{rec}) - \omega t \sin \phi_{rec}], \\ v_{D_r,on} = I_m [\sin(\omega t + \phi_{rec}) - \sin(\phi_{rec})] \cdot r_{D_r}. \quad (7)$$

Based on the proposed analysis in [13], D and ϕ_{rec} can be determined by Kirchoff's voltage law and the switching condition of the diode.

$$C_r = \frac{1 + \frac{[\sin 2\pi D + 2\pi(1-D)]^2}{1 - \cos 2\pi D} - 2\pi^2(1-D)^2 - \cos 2\pi D}{2\pi\omega(R_l + r_{L_r} + r_{D_r})}. \quad (8)$$

$$\tan \phi_{rec} = \frac{1 - \cos 2\pi D}{\sin 2\pi D + 2\pi(1-D)}. \quad (9)$$

Then the input resistance and reactance of the Class E rectifier can be derived as follow

$$R_{rec} = 2\sin^2 \phi_{rec} (R_l + r_{L_r}) + 2er_{D_r} \quad (10)$$

$$X_{rec} = -\frac{1}{\pi} \left[\frac{a+b}{\omega C_r} + r_{D_r}(c+d) \right]. \quad (11)$$

where ω is the operating frequency and

$$a = \pi(1 - D) + 2\pi(1 - D) \sin \phi_{rec} \sin(\phi_{rec} - 2\pi D) \quad (12)$$

$$b = \sin 2\pi D + \frac{1}{4} \sin(2\phi_{rec} - 4\pi D) - \frac{1}{4} \sin 2\phi_{rec}, \quad (13)$$

$$c = \frac{1}{2} - \frac{\cos 2\phi_{rec}}{4} - \frac{\cos(2\phi_{rec} - 4\pi D)}{4}, \quad (14)$$

$$d = -\sin \phi_{rec} \sin(\phi_{rec} - 2\pi D). \quad (15)$$

$$e = \frac{D}{2} + D \sin^2 \phi_{rec} - \frac{1}{\pi} \sin \phi_{rec} \cos(\phi_{rec} - 2\pi D) \\ + \frac{1}{8\pi} \sin(2\phi_{rec} - 4\pi D) + \frac{3}{8\pi} \sin 2\phi_{rec} \quad (16)$$

At last, the efficiency of rectifier is calculated considering the power loss in the on-resistance of diode and ESR of filter inductor [13].

$$\eta_{rec} = \frac{R_L}{R_L + r_{Lr} + \frac{e r_{Dr}}{\sin^2 \phi_{rec}}}, \quad (17)$$

It is clear that the parallel capacitor C_r is the only design parameter, having influence on the efficiency of Class E rectifier.

B. Coupling coils

In the conventional design of coupling coils, the resonance at operating frequency is empirically addressed neglecting the input reactance of rectifier. However, once the operating frequency is as high as several megahertz, the appearance of the rectifier input reactance would greatly detune the resonance between coupling coils. Therefore, the derived input reactance of rectifier in (11) are taken into consideration to retune the coupling coils as shown in Fig. 4. Here, L_{tx} , r_{tx} , L_{rx} and r_{rx} are the self-inductances and self-resistances of the transmitting coil and receiving coil, while C_{tx} and C_{rx} are the in-series compensation capacitances of the coils. The mutual inductance of the coils, i.e. L_m can be derived as

$$L_m = k \sqrt{L_{tx} L_{rx}}, \quad (18)$$

where k is the mutual inductance coefficient.

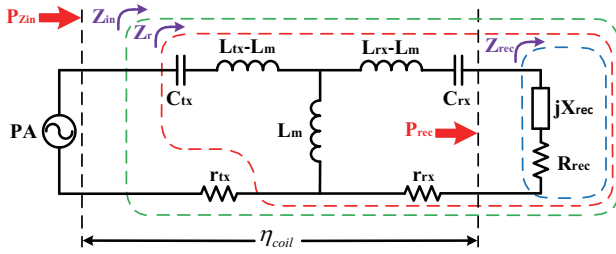


Fig. 4. Circuit model of the coupling coils.

In Fig. 4, the input resistance and reactance of the coupling coils, i.e., R_{coil} and X_{coil} can be derived directly by circuit analysis

$$R_{coil} = \frac{\omega^2 L_m^2 (R_{rec} + r_{rx})}{(R_{rec} + r_{rx})^2 + (X_{rec} + \omega L_{rx} - \frac{1}{\omega C_{rx}})^2} + r_{tx}, \quad (19)$$

$$X_{coil} = \omega L_{tx} - \frac{\omega^2 L_m^2 (X_{rec} + \omega L_{rx} - \frac{1}{\omega C_{rx}})}{(R_{rec} + r_{rx})^2 + (X_{rec} + \omega L_{rx} - \frac{1}{\omega C_{rx}})^2} - \frac{1}{\omega C_{tx}}. \quad (20)$$

The efficiency of the coupling coils can be determined in consideration of the in-series power loss in r_{tx} and r_{rx} ,

$$\eta_{coil} = \frac{R_{coil} - r_{tx}}{R_{coil}} \cdot \frac{R_{coil}}{R_{coil} + r_{rx}} \quad (21)$$

Combining (17) and (21) yields the efficiency and power factor of the entire WPT system in Fig. 1.

$$\eta = \eta_{coil} \cdot \eta_{rec}, \quad (22)$$

$$PF = \frac{R_{coil}}{\sqrt{R_{coil}^2 + X_{coil}^2}}. \quad (23)$$

C. Variation of model parameters

Based on the previous discussion, the efficiency of the WPT system, i.e. η in (22), can be analytically addressed using static circuit equations. But some parameter variations are commonly existed and difficult to measure in various applications, including the misalignment of coupling coils and change of DC load. Meanwhile, the equivalent resistance of the rectifying diode under the different power level is another well accepted variable. Besides the efficiency of WPT system, its robustness against variations is another common evaluation of the system design that is equally important. For the ease of formulation, it is a reasonable approach to equate the unpredictable variations by interval-based parameter uncertainties. Then, the proposed WPT system can be formulated by static circuit equations with uncertain parameters.

Indeed, the misalignment of coupling coils and change of DC load are represented as variations of mutual inductance coefficient k and load resistance R_l , whose variation ranges are also specified as

$$k_{min} \leq k \leq k_{max}, \quad R_{lmin} \leq R_l \leq R_{lmax}. \quad (24)$$

The equivalent resistance of the rectifying diode changes under different power level due to the existence of the forward voltage drop V_{drop} during the on-state of diode, which is usually regarded as a constant value. Suppose the on-state root mean square (RMS) current cross the rectifying diode is $I_{Dr, rms}$, the equivalent resistance of the diode, i.e., r_{Dr} can be obtained as shown in Fig. 5.

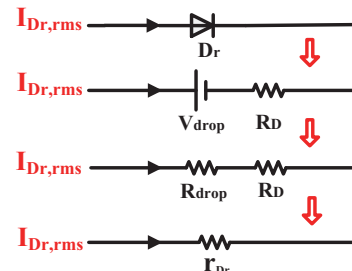


Fig. 5. Equivalence of the rectifying diode in its on-state.

Indeed, the following equations are assumed in the on-state of diode.

$$\begin{aligned} V_{drop} &= I_{D_r, rms} \cdot R_{drop}, \\ r_{D_r} &= R_{drop} + R_D, \end{aligned} \quad (25)$$

where R_{drop} can be considered as the virtual resistance resulting from the forward voltage drop V_{drop} . It is a reasonable linear approach to represent r_{D_r} as

$$r_{D_r} = R_D + \frac{V_{drop}}{I_{D_r, rms}}. \quad (26)$$

Once the current across the diode is represented in (5), the RMS current $I_{D_r, rms}$ can be derived using

$$I_{D_r, rms} = \sqrt{\frac{1}{2\pi D} \int_{2\pi(1-D)}^{2\pi} i_{D_r}^2 d\omega t} \quad (27)$$

The representation of $I_{D_r, rms}$ is shown in (28) which is a function of not only the circuit parameters but also the input current of rectifier, i.e., I_m in (1). Now that in (25), even V_{drop} and R_D are constant parameters, the value of r_{D_r} will oscillate with respect to the change of system power level. Then, the impact of power level can be uniquely embodied to its influence on equivalent resistance of the diode. In order for a robust design against power difference, r_{D_r} is also equivalently defined as an uncertainty with variation interval.

$$(r_{D_r})_{min} \leq r_{D_r} \leq (r_{D_r})_{max}. \quad (29)$$

III. OPTIMIZATION PROBLEM

Combining (8)-(23), the efficiency η and power factor PF of system can be regarded as derived functions of all the circuit parameters including

$$\{\omega, L_{tx}, r_{tx}, L_{rx}, r_{rx}, r_{L_r}, k, R_l, r_{D_r}, C_{tx}, C_{rx}, C_r\}. \quad (30)$$

The design variables \mathbf{X} of the overall system include the in-series compensation capacitors of the coils and the parallel capacitor of the rectifier.

$$\mathbf{X} = (C_{tx}, C_{rx}, C_r). \quad (31)$$

The operating frequency and all the inductive coils are assumed predefined with constant parameters $\bar{\mathbf{P}}$.

$$\bar{\mathbf{P}} = (\omega, L_{tx}, r_{tx}, L_{rx}, r_{rx}, r_{L_r}). \quad (32)$$

While the uncertain parameters discussed in Section II-C are defined as $\tilde{\mathbf{P}}$.

$$\tilde{\mathbf{P}} = (k, R_l, r_{D_r}). \quad (33)$$

whose variation range is restricted to

$$\begin{aligned} \tilde{\mathbf{P}} &\in (\tilde{\mathbf{P}}_{min}, \tilde{\mathbf{P}}_{max}) \\ \tilde{\mathbf{P}}_{min} &= (k_{min}, R_{lmin}, (r_{D_r})_{min}), \\ \tilde{\mathbf{P}}_{max} &= (k_{max}, R_{lmax}, (r_{D_r})_{max}). \end{aligned} \quad (34)$$

The efficiency and power factor of the overall system can be represented as functions of design variables \mathbf{X} , constant parameters $\bar{\mathbf{P}}$ and uncertain parameters $\tilde{\mathbf{P}}$.

$$\eta = \eta(\mathbf{X}, \bar{\mathbf{P}}, \tilde{\mathbf{P}}), \quad (35)$$

$$PF = PF(\mathbf{X}, \bar{\mathbf{P}}, \tilde{\mathbf{P}}), \quad (36)$$

Suppose the nominal values of the uncertain parameters $\tilde{\mathbf{P}}$ is $\tilde{\mathbf{P}}_0$, the efficiency and power factor for system with $\tilde{\mathbf{P}}_0$, i.e., nominal efficiency and power factor, are defined as η_0 and PF_0 which are only functions of design variables \mathbf{X} .

$$\eta_0 = \eta_0(\mathbf{X}) = \eta(\mathbf{X}, \bar{\mathbf{P}}, \tilde{\mathbf{P}}_0), \quad (37)$$

$$PF_0 = PF_0(\mathbf{X}) = PF(\mathbf{X}, \bar{\mathbf{P}}, \tilde{\mathbf{P}}_0), \quad (38)$$

A. Objective function

The optimization of the proposed WPT system searches for the highest efficiency by proper assignment of the design variables in (31). So the objective function $f(\mathbf{X})$ is selected as the nominal efficiency η_0 defined in (37),

$$f(\mathbf{X}) = \eta_0(\mathbf{X}) = \eta(\mathbf{X}, \bar{\mathbf{P}}, \tilde{\mathbf{P}}_0), \quad (39)$$

Then, the optimization result \mathbf{X}^* corresponds to the maximum of $f(\mathbf{X})$ in subject to the following constraints on robustness and power factor.

B. Constraint on robustness

The robustness of a WPT system design can be described as the variation of its efficiency with respect to the variations of working condition, i.e. uncertain parameters. The robust optimization tends to find an optimal solution that the value of objective function is insensitive to the variation uncertain parameters. Indeed, the constraint on robustness is defined that the proportional variation of the efficiency $\eta(\mathbf{X}, \bar{\mathbf{P}}, \tilde{\mathbf{P}})$ with respect to the variations of $\tilde{\mathbf{P}}$ should be restricted to an acceptable range, i.e., the robust index ϵ , which is usually based on specific requirement of a designer.

$$\max_{\tilde{\mathbf{P}}} \left| \frac{\eta(\mathbf{X}, \bar{\mathbf{P}}, \tilde{\mathbf{P}}) - \eta(\mathbf{X}, \bar{\mathbf{P}}, \tilde{\mathbf{P}}_0)}{\eta(\mathbf{X}, \bar{\mathbf{P}}, \tilde{\mathbf{P}}_0)} \right| \leq \epsilon. \quad (40)$$

In (40), smaller value of ϵ always corresponds to higher requirement on robustness.

C. Constraint on power factor

For a WPT system with higher power factor, lower input voltage source is required to achieve a same power level on the load. In this proposed topology, the power factor PF should be limited to avoid the appearance of high peak voltage in the output of power amplifier in Fig. 1. Here, the uncertainties of working conditions are also considered to guarantee sufficient power factor under any possible parameter variations.

$$\min_{\tilde{\mathbf{P}}} PF(\mathbf{X}, \bar{\mathbf{P}}, \tilde{\mathbf{P}}) \geq \delta. \quad (41)$$

Similarly, δ is defined as the power factor index, which is based on the design of power amplifier and requirement of power level on the load. And larger value of δ in (41) always represents higher requirement on power factor.

$$I_{D_r,rms} = I_m \sqrt{\frac{4\pi D + 8\pi D \sin^2 \phi_{rec} + 3\sin(2\phi_{rec}) + \sin(2\phi_{rec} - 4\pi D) - 8\sin\phi_{rec}\cos(\phi_{rec} - 2\pi D)}{8\pi D}}. \quad (28)$$

D. Problem formulation and solution

Combining the objective function in (39), the constraints in (40), (41) and the uncertainties of circuit parameters in (34), the entire robust optimization problem can be defined as:

$$\begin{aligned} \min_{\mathbf{X}} \quad & f(\mathbf{X}) = \eta_0(\mathbf{X}) = \eta(\mathbf{X}, \bar{\mathbf{P}}, \tilde{\mathbf{P}}_0), \\ \text{s.t.} \quad & \max_{\tilde{\mathbf{P}}} \left| \frac{\eta(\mathbf{X}, \bar{\mathbf{P}}, \tilde{\mathbf{P}}) - \eta(\mathbf{X}, \bar{\mathbf{P}}, \tilde{\mathbf{P}}_0)}{\eta(\mathbf{X}, \bar{\mathbf{P}}, \tilde{\mathbf{P}}_0)} \right| \leq \epsilon, \\ & \min_{\tilde{\mathbf{P}}} PF(\mathbf{X}, \bar{\mathbf{P}}, \tilde{\mathbf{P}}) \geq \delta \end{aligned}$$

$$\text{where } \tilde{\mathbf{P}} \in (\tilde{\mathbf{P}}_{min}, \tilde{\mathbf{P}}_{max}). \quad (42)$$

In (42), the uncertain parameters exist in both constraint functions. This parameter variation in optimization would lead to a nested optimization structure. It can be seen that each constraint function includes a so-called inner optimization with respect to the variations of circuit parameters $\tilde{\mathbf{P}}$. Here, the inner optimizations are used to guarantee enough robustness on efficiency while the constraint on power factor is not violated under any possible variation of circuit parameters $\tilde{\mathbf{P}}$. Meanwhile, the outer optimization evaluates the performance of each candidate solution \mathbf{X} using the objective function with nominal values of uncertain parameters. It is a typical robust optimization problem which can be solved via inner-outer optimization algorithms [14].

In this work, both the formulations in inner and outer optimizations are not differentiable, where one intermediate variable called duty cycle of diode, i.e. D in (8) is even represented by an implicit function. It is a common sense that gradient-based optimization algorithms are unable to address the global optimum for problems with undifferentiable and implicit objective and constraint functions. Instead, genetic algorithm (GA) is applied to solve both the inner and outer optimization. GA is one of the most popular population-based heuristic approach, which could find the global or at least near-to-global optimum. In consideration of the nature of the robust optimization problem in (42), GA is an appropriate solver to address the global optimal solution.

For each candidate \mathbf{X} generated by the outer optimization in (42), its feasibility will be checked in each constraint with respect to the variation of $\tilde{\mathbf{P}}$, where this \mathbf{X} is treated as a vector of constants and considered feasible only if both the constraints are satisfied. In this way, the achieved optimal solution not only has the best objective function value, i.e. highest power efficiency, among all the feasible candidate solutions, but also robust in terms of efficiency and power factor.

IV. DESIGN CASE

Based on the analytical derivation of WPT system, the parameter design for a 6.78-MHz WPT system is discussed.

The values of all the constant parameters $\bar{\mathbf{P}}$ in (42) are specified in Table. I, while the nominal values and variation range of all the uncertain parameters $\tilde{\mathbf{P}}$ are listed in Table. II.

According to (26), the variation of r_{D_r} depends on the RMS current across the diode. With respect to the voltage drop V_{drop} and the on-resistance R_D in Table. I, the variation range of r_{D_r} in Table. II is selected in corresponds to a wide range of input current.

$$r_{D_r} \in [0.7, 1.9] \quad (43)$$

It implies

$$I_{D_r,rms} \in [1.0, 4.0]. \quad (44)$$

Note the $I_{D_r,rms}$ is closely related to the power level of the system. And the nominal value of r_{D_r} , i.e., 1.3Ω corresponds to a rated RMS current of $1.6 A$.

The power factor index δ is selected to be 0.3 in Table. I as an example. Now that by assigning different values to the robust index ϵ , a robust optimization problem denoted by (42) can be specified to address the optimal solutions of the design variables \mathbf{X} .

TABLE II
PARAMETERS WITH VARIED VALUES

$\tilde{\mathbf{P}}$	k	$R_l(\Omega)$	$r_{D_r}(\Omega)$
Lower limits ($\tilde{\mathbf{P}}_{min}$)	0.1	10	0.7
Nominal values ($\tilde{\mathbf{P}}_0$)	0.2	50	1.3
Upper limits ($\tilde{\mathbf{P}}_{max}$)	0.3	100	1.9

Using robust optimization algorithm, the design results of \mathbf{X} and the resulting nominal efficiency η_0 , i.e., the value of objective function, is listed in Table. III, where the robust index, ϵ is numerated from 0.15 to 0.25. It can be seen that smaller value of robust index always leads to lower overall efficiency, i.e., the value of cost function. The reason is that a smaller value of ϵ always corresponds to higher requirement of robustness. And the trade-off between robustness requirement and optimal solution always exists in robust optimization problem.

TABLE III
PARAMETER DESIGN FOR A VARIABLE ROBUST INDEX

ϵ	$C_{tx}(pF)$	$C_{rx}(pF)$	$C_r(pF)$	η_0
0.150	152.2	190.4	471.5	86.33%
0.175	185.2	198.0	416.1	87.22%
0.200	154.9	198.7	309.3	89.08%
0.225	160.0	190.0	180.9	90.79%
0.250	166.1	210.2	62.2	91.93%

As an example, the robust index ϵ is selected as 0.2 in the following experiment, which means that the variation of system efficiency is required to be within 20 percent for any possible value of uncertain parameters in Table. II. Based on Table. III, the parameters used in experiment are

$$[C_{tx}, C_{rx}, C_r] = [154.9pF, 198.7pF, 309.3pF]. \quad (45)$$

TABLE I
PARAMETERS WITH CONSTANT VALUES

$\omega(\text{MHz})$	$L_{tx}(\mu\text{H})$	$r_{tx}(\Omega)$	$L_{rx}(\mu\text{H})$	$r_{rx}(\Omega)$	$r_{Lr}(\Omega)$	$V_{drop}(\text{V})$	$R_D(\Omega)$	δ
6.78	3.34	0.7	3.34	0.7	0.2	1.6	0.3	0.3

And the theoretical value of nominal efficiency is

$$\eta_0 = 89.13\%. \quad (46)$$

Before experiment, calculation results are carried out in Fig. 6 for the efficiency and power factor with dual variations among mutual inductance coefficient k , load resistance R_l , and equivalent resistance of diode r_{D_r} . The nominal condition, $\bar{P}_0 = (k_0, R_{l0}, r_{D_r,0})$ is marked by a red circle in all the surfaces.

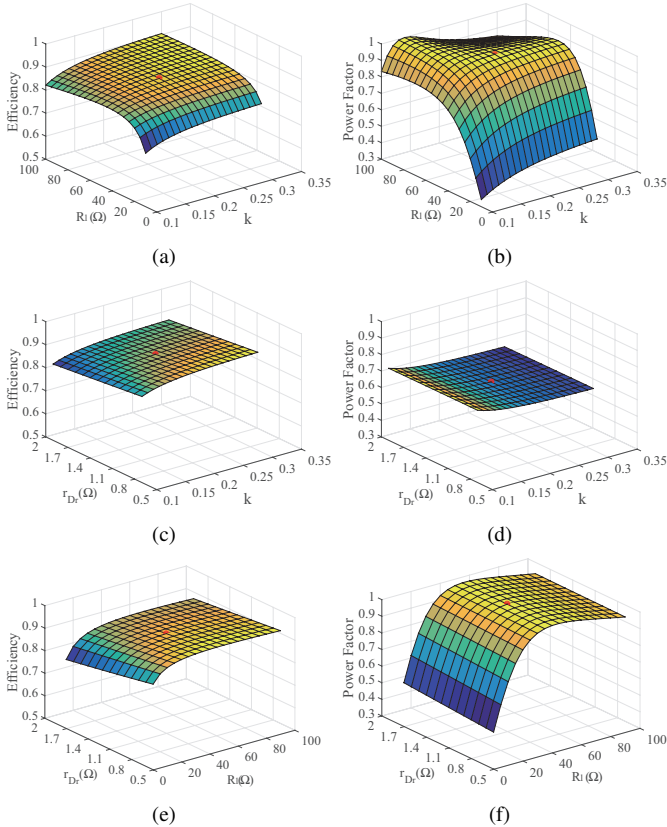


Fig. 6. The calculation results based on analytical derivation. (a) Efficiency with variations of k and R_l when $r_{D_r} = 1.3 \Omega$. (b) Power factor with variations of k and R_l when $r_{D_r} = 1.3 \Omega$. (c) Efficiency with variations of k and r_{D_r} when $R_l = 50 \Omega$. (d) Power factor with variations of k and r_{D_r} when $R_l = 50 \Omega$. (e) Efficiency with variations of R_l and r_{D_r} when $k = 0.2$. (f) Power factor with variations of R_l and r_{D_r} when $k = 0.2$.

It can be seen that the efficiency has a strong robustness against the variations of parameters, while the constraint on power factor is not violated. Referring to Fig. 6(a)(c), the decrease of mutual inductance coefficient k would lead to the decrease of the efficiency. The reason is that smaller k would lead to a smaller input resistance of the coupling coils, i.e. R_{coil} in (19), which would lead to higher power loss on the in-series self-resistance of the transmitting coil r_{tx} as indicated in (21). Meanwhile, The load resistance is found to have strong impact on the power factor of the system as

shown in Fig. 6(b)(f). Smaller load resistance represents higher input reactance of the coupling coils, which contributes to the decline of power factor. In addition, the change of r_{D_r} would lead to larger variation of efficiency for system with smaller load resistance as shown in Fig. 6(e). It is because more power would be delivered to the diode with the decreasing of load resistance based on (17).

In summary, the calculation results in Fig. 6 can match the theoretical discussions above and reflect the fundamental properties of WPT system, which verify that the proposed design in (47) is a satisfactory solution of the robust optimization problem.

V. EXPERIMENTAL VERIFICATION

A 6.78-MHz WPT system is built up to verify the above analytical derivations and parameter design via robust optimization. This experimental system shares the same circuit configuration with the one in Fig. 1. The power level of the WPT system at the nominal work condition ($k = 0.2$, $R_l = 50 \Omega$, $r_{D_r} = 1.3 \Omega$) is 5W in the experiments. The robust index ϵ and power factor index δ are selected to be 0.2 and 0.5 as the examples, respectively. Based on the proposed robust optimization given in section III, the optimal results X^* used in the experiment is calculated as follows,

$$[C_{tx}, C_{rx}, C_r] = [154.9\text{pF}, 198.7\text{pF}, 309.3\text{pF}]. \quad (47)$$

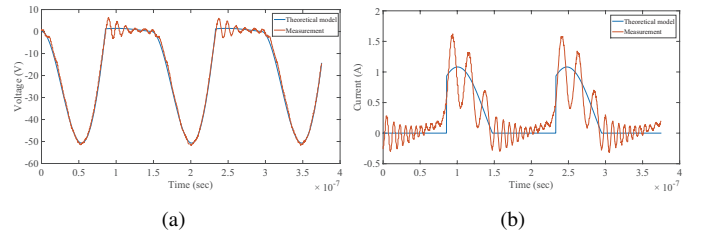


Fig. 7. Experimental and theoretical waveforms of the Class E current-driven rectifier. (a) Diode voltage. (b) Diode current.

Fig. 7 shows the experimental results of the waveforms of the Class E rectifier. The theoretical results of the diode waveforms are also referred for comparison in Fig. 7. It can be seen that the voltage waveform in experiment can well match the theoretical derivation. The oscillation of the diode current in experiment is due to the lead inductance of the additional wire on the pin of the diode during the current measurement. After the validation of rectifier performance, the efficiency of the overall system is also carried out in experiment in consideration of the variation of working conditions. As a realization in experiment, k is varied by adjusting the distance between coils and R_l is tuned by adjusting the electronic load. In the experiments, the varying k and R_l lead to the varying

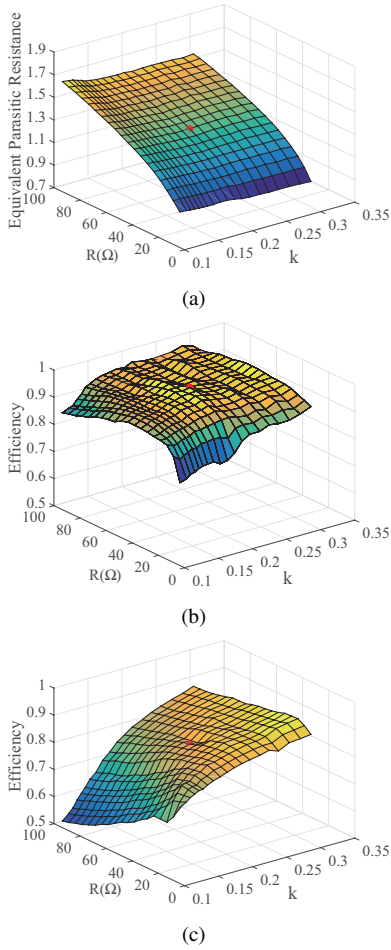


Fig. 8. Experimental results. (a) The variation of r_{D_r} . (b) Efficiency in the proposed robust design. (c) Efficiency in the conventional design.

input power of the WPT system and then the varying r_{D_r} as shown in Fig. 8 (a). The experimental efficiency of the WPT system using the robust optimization is measured as a surface in Fig. 8 (b) under different mutual inductance and load resistance, where the efficiency under nominal condition is also marked as a red circle. For the comparison purpose, the efficiency of the conventional design is also shown in Fig. 8 (c). It can be seen that the proposed robust optimization is superior both in terms of the efficiency and robustness. All experimental results above indicate that the proposed design using robust optimization can provide a stable system with respect to the variation of parameters (k , R_l , r_{D_r}).

VI. CONCLUSIONS

This paper discusses the design of a WPT system with the Class E rectifier. Both the efficiency and robustness of the WPT system are emphasized to meet the common requirements in real applications. The overall system is first solved as circuit equations through analytical derivation. Specifically, the mutual inductance coefficient, load resistance, and equivalent resistance of diode are regarded as uncertain parameters in consideration of the robustness against the variation of working conditions. The system parameters design is then formulated as a robust optimization problem in search for the

optimal efficiency with constraints on power factor and robustness. Both the calculation and experimental results validate the outstanding performance of the proposed system design in comparison with the conventional design for the MHz WPT system. The successful application of robust optimization for the 6.78-MHz WPT system indicates its feasibility and potential on power system design.

REFERENCES

- [1] A. Kurs, A. Karalis, R. Moffatt, J. D. Joannopoulos, P. Fisher, and M. Soljačić, "Wireless power transfer via strongly coupled magnetic resonances," *science*, vol. 317, no. 5834, pp. 83–86, July 2007.
- [2] S. Hui, W. Zhong, and C. Lee, "A critical review of recent progress in mid-range wireless power transfer," *IEEE Trans. Power Electron.*, vol. 29, no. 9, pp. 4500–4511, Sept 2014.
- [3] W. Zhong, C. Zhang, X. Liu, and S. Hui, "A methodology for making a three-coil wireless power transfer system more energy efficient than a two-coil counterpart for extended transfer distance," *IEEE Trans. Power Electron.*, vol. 30, no. 2, pp. 933–942, Feb 2015.
- [4] M. Pinuela, D. C. Yates, S. Lucyszyn, and P. D. Mitcheson, "Maximizing DC-to-load efficiency for inductive power transfer," *IEEE Trans. Power Electron.*, vol. 28, no. 5, pp. 2437–2447, May 2013.
- [5] A. Sample, B. Waters, S. Wisdom, and J. Smith, "Enabling seamless wireless power delivery in dynamic environments," *Proc. IEEE*, vol. 101, no. 6, pp. 1343–1358, June 2013.
- [6] S.-H. Lee and R. D. Lorenz, "Development and validation of model for 95%-efficiency 220-w wireless power transfer over a 30-cm air gap," *IEEE Trans. Appl. Ind.*, vol. 47, no. 6, pp. 2495–2504, Nov 2011.
- [7] S. Aldhaher, P.-K. Luk, and J. F. Whidborne, "Electronic tuning of misaligned coils in wireless power transfer systems," *IEEE Trans. Power Electron.*, vol. 29, no. 11, pp. 5975–5982, Nov 2014.
- [8] S. Aldhaher, P.-K. Luk, A. Bati, and J. Whidborne, "Wireless power transfer using Class E inverter with saturable DC-feed inductor," *IEEE Trans. Ind. Appl.*, vol. 50, no. 4, pp. 2710–2718, July 2014.
- [9] M. Fu, H. Yin, X. Zhu, and C. Ma, "Analysis and tracking of optimal load in wireless power transfer systems," *IEEE Trans. Power Electron.*, vol. 30, no. 7, pp. 3952–3963, July 2015.
- [10] M. Fu, T. Zhang, C. Ma, and X. Zhu, "Efficiency and optimal loads analysis for multiple-receiver wireless power transfer systems," *IEEE Trans. Microw. Theory Tech.*, vol. 63, no. 3, pp. 801–812, March 2015.
- [11] S. Aldhaher, P.-K. Luk, K. El Khamlichy Drissi, and J. Whidborne, "High-input-voltage high-frequency Class E rectifiers for resonant inductive links," *IEEE Trans. Power Electron.*, vol. 30, no. 3, pp. 1328–1335, March 2015.
- [12] P.-K. Luk, S. Aldhaher, W. Fei, and J. Whidborne, "State-space modeling of a Class E^2 converter for inductive links," *IEEE Trans. Power Electron.*, vol. 30, no. 6, pp. 3242–3251, June 2015.
- [13] M. Liu, M. Fu, and C. Ma, "Parameter design for a 6.78-mhz wireless power transfer system based on analytical derivation of class e current-driven rectifier," 2015.
- [14] M. Li, S. Azarm, and A. Boyars, "A new deterministic approach using sensitivity region measures for multi-objective robust and feasibility robust design optimization," *Journal of mechanical design*, vol. 128, no. 4, pp. 874–883, 2006.